Journal of Photochemistry and Photobiology A: Chemistry 229 (2012) 20–28

Contents lists available at SciVerse ScienceDirect

Journal of Photochemistry and Photobiology A: Chemistry

journal homepage: www.elsevier.com/locate/jphotochem

Synthesis and properties of molecular switches based on the opening and closing of oxazine rings

Erhan Deniz[a], Janet Cusido[a], Subramani Swaminathan[a], Mutlu Battal[a], Stefania Impellizzeri[a], Salvatore Sortino[b,*], Françisco M. Raymo[a,*]

[a] Laboratory for Molecular Photonics, Department of Chemistry, University of Miami, 1301 Memorial Drive, Coral Gables, FL 33146-0431, United States
[b] Laboratory of Photochemistry, Department of Drug Sciences, University of Catania, Viale Andrea Doria 6, I-95125 Catania, Italy

ARTICLE INFO

Article history:
Received 19 October 2011
Received in revised form
19 November 2011
Accepted 26 November 2011
Available online 8 December 2011

Keywords:
Fluorescence
Halochromism
Molecular switches
Oxazines
Photochromism

ABSTRACT

We designed and synthesized a family of molecular switches each pairing an oxazine ring to a chromophoric fragment. Under the influence of either chemical or optical stimulations, the oxazine ring opens to bring the chromophoric appendage in conjugation with either a 3*H*-indolium cation or a phenolate anion. These structural transformations alter the electronic structure of the chromophore and, as a result, its electrochemical and spectroscopic signatures. Specifically, we demonstrated that the absorption of triphenylamine and thiophene fragments, the fluorescence of a coumarin appendage and the oxidation potential of a ferrocene center can all be switched with acid, base or ultraviolet inputs. Thus, these operating principles and structural designs for switching properties at the molecular level with the aid of external stimulations might eventually lead to a general strategy for the realization of chemo- and photo-responsive materials.

1. Introduction

Organic molecules can be designed to undergo pronounced structural changes in response to external stimulations [1]. In turn, these switching events can be exploited to control motion at the molecular level as well as to regulate the electrochemical and spectroscopic signatures of multicomponent assemblies [2]. Indeed, molecular switches are becoming valuable building blocks for the construction of a diversity of functional materials with controllable properties. In particular, photochromic switches offer the opportunity to implement such structural transformations reversibly under the influence of light [3–8]. The photochemical events associated with these compounds can be accompanied by significant changes in absorption coefficients, dipole moments, fluorescence quantum yields and redox potentials together with pronounced modifications in molecular shapes and dimensions. In fact, the ability to photoregulate these parameters has already translated into the realization of photoresponsive molecular and supramolecular constructs based on photochromic components [9–14].

In search of strategies to implement photochromic transformations with fast switching speeds, we developed a family of oxazines able to open and close their heterocyclic core in response to optical stimulations [15]. Specifically, our molecules fuse 2*H*,3*H*-indole and 2*H*,4*H*-benzo[1,3]oxazine heterocycles in their molecular skeletons. Upon ultraviolet illumination, the [C—O] bond at the junction of the two heterocycles cleaves on a subnanosecond timescale. The photoinduced bond cleavage opens the oxazine ring and generates a phenolate chromophore. As a result, this photochemical process is accompanied by the appearance of an absorption band in the visible region of the electromagnetic spectrum. The photogenerated isomer, however, reverts spontaneously to the original one on a submicrosecond timescale. Indeed, these molecules can be switched back and forth between their two interconvertible states hundreds of times with no sign of degradation, even in the presence of molecular oxygen.

In the course of investigating the photochemical and photophysical properties of our photochromic compounds, we discovered that their oxazine ring opens also under the influence of either acid or base with the formation of either a 3*H*-indolium or a phenolate chromophore respectively [15a,g]. As a result, these transformations are, once again, accompanied by significant changes in absorption across the ultraviolet and visible regions of the electromagnetic spectrum. On the basis of these observations, we envisaged the opportunity of exploiting the halochromic and photochromic character of our relatively simple switching subunit to control the properties of an appended component. Specifically, we devised versatile synthetic strategies to attach covalently an oxazine ring to a diversity of chromophoric groups with the ultimate goal of being able to modulate their absorption,

* Corresponding authors.
E-mail addresses: ssortino@unict.it (S. Sortino), fraymo@miami.edu (F.M. Raymo).

1010-6030/$ – see front matter © 2011 Elsevier B.V. All rights reserved.
doi:10.1016/j.jphotochem.2011.11.008

electrochemical and/or emission properties under the influence of light, acid and/or base. In order to assess the generality of these operating principles, we designed eight molecular switches all pairing covalently an oxazine ring to an appropriate chromophore. In this article, we report the synthesis of these molecules and of appropriate models together with the electrochemical, photochemical and photophysical properties of these functional compounds.

2. Results and discussion

2.1. Design and synthesis

The photoinduced opening (from ***a*** to ***b*** in Fig. 1) of the oxazine ring of our photochromic compounds generates a zwitterionic isomer incorporating a phenolate anion and a 3*H*-indolium cation

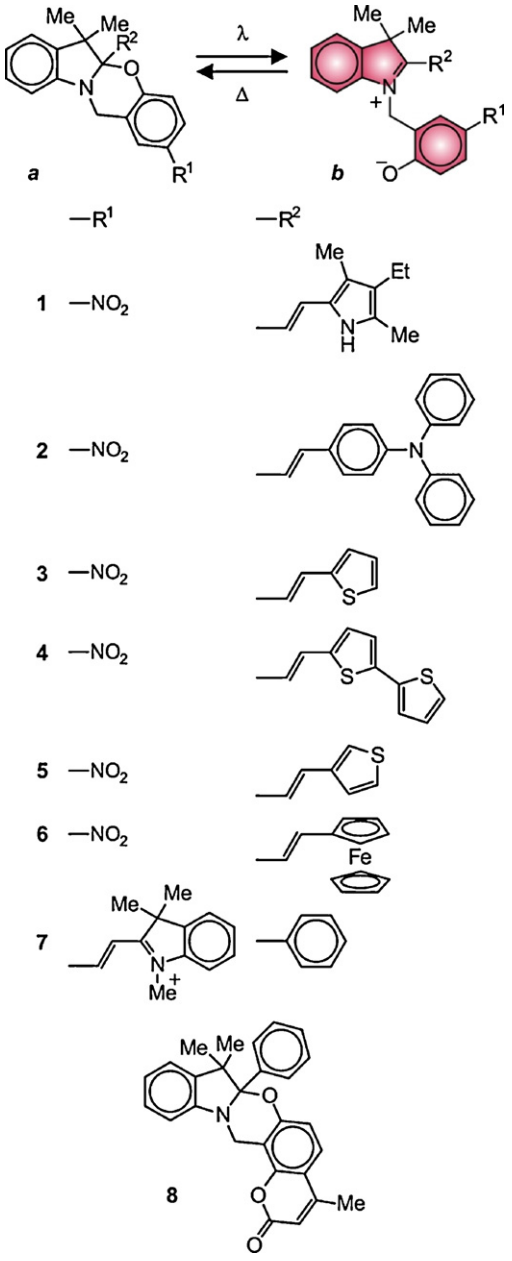

Fig. 1. The molecular switches **2**–**8** adopt preferentially a ring-closed form (***a***) in solution, while **1** is exclusively in the ring-open state (***b***) under the same conditions. The oxazines **2a**, **3a** and **5a** switch reversibly to the corresponding zwitterionic isomers **2b**, **3b** and **8b** upon ultraviolet illumination. Instead, **4a** and **6a**–**8a** do not undergo this photochemical transformation.

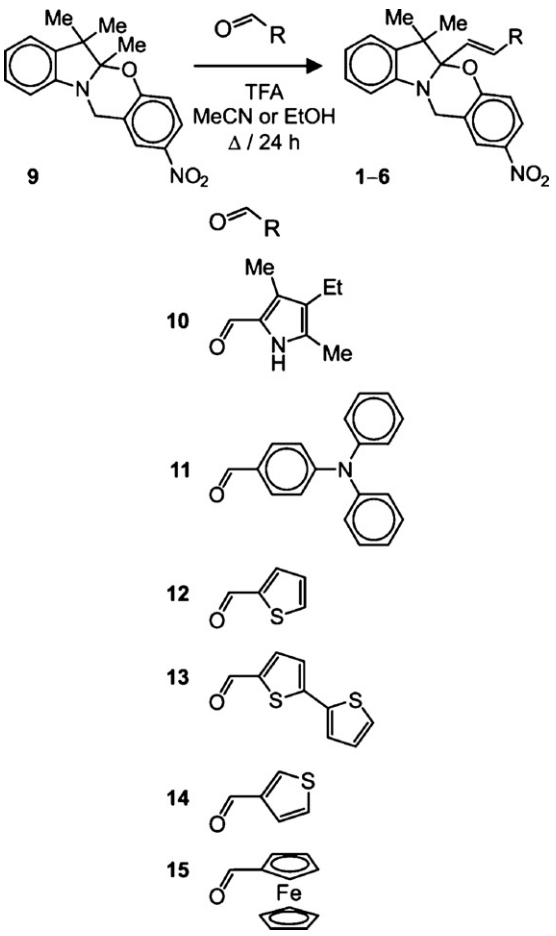

Fig. 2. Synthesis of the molecular switches **1**–**6**.

[15]. This transformation can be exploited to perturb the electronic structure of a chromophoric appendage attached to either position 4 on the phenoxy fragment (R^1 in Fig. 1) or the chiral center at the junction of the two heterocycles (R^2 in Fig. 1). Indeed, the developing charges on the phenolate and 3*H*-indolium fragments can donate electrons to R^1 and withdraw them from R^2 respectively. Thus, the photoinduced opening and thermal closing of the oxazine ring can, in principle, be exploited to modulate the absorption, emission and redox properties of a chromophore attached to either one of these two positions. On the basis of these considerations and the availability of appropriate precursors, we designed the molecular switches **1**–**8** (Fig. 1) and devised synthetic procedures for their preparation in a single step from known starting materials with yields ranging from 16% to 46%. In particular, we condensed the preformed oxazine **9** with the aldehydes **10**–**15** (Fig. 2) in the presence of trifluoroacetic acid (TFA) to generate the target switches **1**–**6**. Similarly, we condensed the preformed oxazine **16** (Fig. 3) with the iodide salt of **17** and isolated the hexafluorophosphate salt of the target switch **7**, after counterion exchange. In the case of **8**, instead, we reacted the coumarin **18** (Fig. 4) with formaldehyde and hydrochloric acid first and then with the 3*H*-indole **19** to produce the target switch.

In addition to the molecular switches **1**–**8**, we also synthesized the model compounds **20**–**24**, **26** and **27** (Fig. 5). Specifically, we isolated the hexafluorophosphate salts of these 3*H*-indolium cations in yields ranging from 24% to 85%, after the condensation of the iodide salt of **17** to the corresponding aldehydes and counterion exchange. Compounds **20**–**24** have essentially the same chromophoric fragment of the ring-open isomer (***b*** in Fig. 1) of the molecular switches **1**–**5**. Similarly, the model **26** and the conjugate base of the phenol

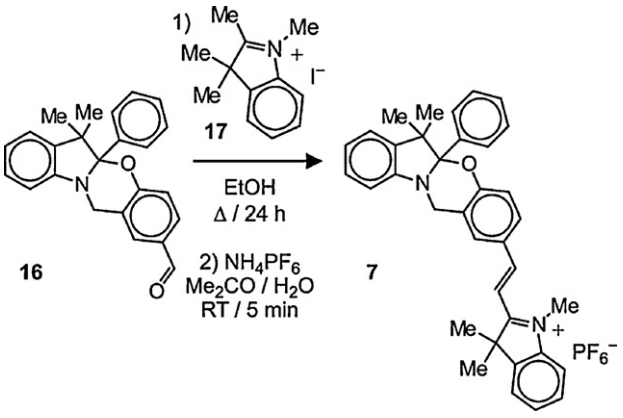

Fig. 3. Synthesis of the molecular switch **7**.

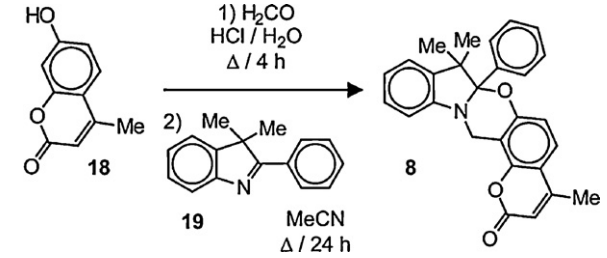

Fig. 4. Synthesis of the molecular switch **8**.

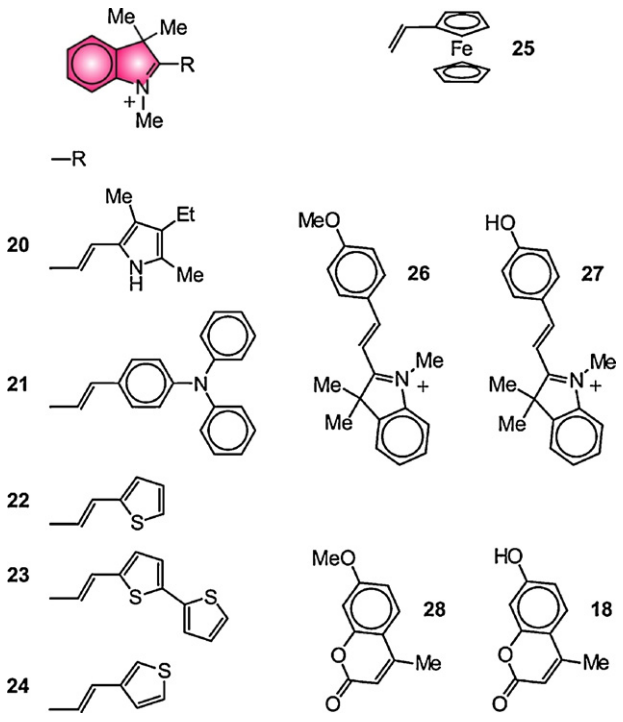

Fig. 5. Model compounds **18** and **20**–**28**.

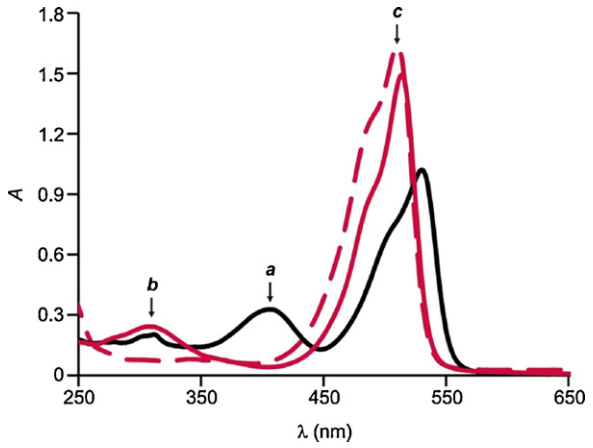

Fig. 6. Steady-state absorption spectra (50 μM, MeCN, 20 °C) of **1** before (***a***) and after (***b***) the addition of TFA (5 equiv.) and of **20** (***c***).

27 resemble the chromophores incorporated within the ring-closed and -open isomers (***a*** and ***b*** in Fig. 1) of **7**.

2.2. Steady-state spectroscopy

The steady-state absorption spectrum of **1** (***a*** in Fig. 6), recorded in acetonitrile at 20 °C, indicates that its ring-open isomer (***b*** in Fig. 1) is the predominant species in solution. Specifically, the spectrum shows the characteristic absorbance of the 4-nitrophenolate chromophore [15a] of this isomer at 408 nm. This band shifts to 307 nm (***b*** in Fig. 6) after the addition of acid and the formation of a 4-nitrophenol chromophore (***c*** in Fig. 7) [15g]. In addition, both spectra show also an intense absorption at *ca.* 530 nm (λ_{Ab} in Table 1). This band resembles that of the model compound **20** and corresponds to the 3*H*-indolium chromophore incorporated within both the ring-open isomer (***b*** in Fig. 1) and its protonated form (***c*** in Fig. 7). These observations demonstrate that the pyrrole fragment of **1** locks this particular system in the ring-open form. Presumably, the extended conjugation of the 3*H*-indolium cation, possible only within the ring-open isomer, is mostly responsible for the preferential population of this species over the ring-closed one.

In contrast to the behavior of **1**, the spectra of **2**–**6** (***a*** in Figs. 8 and S1–S4) indicate that the ring-closed isomer (***a*** in Fig. 1) is, instead, the predominant species in solution, under otherwise identical conditions. The corresponding spectra reveal bands for the chromophore (R^2 in Fig. 1) appended to the chiral center of the oxazine ring at wavelengths ranging from 288 to 337 nm (Table 1). Upon addition of acid, the oxazine ring opens and brings R^2 in conjugation with the adjacent 3*H*-indolium cation in the resulting protonated species (***c*** in Fig. 7). This transformation shifts bathochromically the absorption band of R^2 into the visible region (***b*** in Figs. 8 and S1–S4). In fact, the resulting absorptions resemble those of the model 3*H*-indolium cations **21**–**24** (***c*** in Figs. 8 and S1–S3), which are centered at wavelengths ranging from 400 to 529 nm (Table 1). Thus, the acid-induced opening of the oxazine rings of **2**–**6** alters the electronic structure of their chromophoric appendages and shifts their

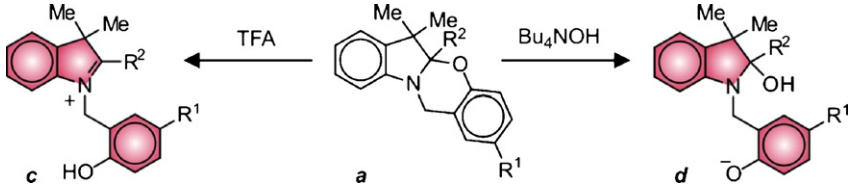

Fig. 7. Opening of the oxazine ring with the addition of either acid or base.

Table 1
Photochemical and photophysical parameters [a] of the ring-open isomer of **1**, ring-closed isomers of **2**–**8** and their models **18** and **20**–**27**.

	λ_{Ab} [b] (nm)	ϕ_P [c]	τ_P [d] (μs)		λ_{Ab} [b] (nm)
1b	530	–	–	**20**	510
2a	326	0.03	0.2	**21**	529
3a	288	0.01	32	**22**	400
4a	337	–	–	**23**	493
5a	316	0.01	50	**24**	382
6a	316	–	–	**25**	275
7a	428	–	–	**27** [e]	538
8a	320	–	–	**18** [e]	388

[a] All parameters were measured in MeCN at 20 °C. [b] The absorption wavelength (λ_{Ab}) was estimated from the spectra in Figs. 6, 8, 9 and S1–S5. [c] The quantum yield (ϕ_P) for the photochromic transformation was determined with a benzophenone standard, following a literature protocol (Ref. [15k]). [d] The lifetime (τ_P) of the photogenerated isomer was determined from the temporal absorbance evolutions in Figs. 10, S6 and S8. [e] The values of λ_{Ab} reported for **27** and **18** were measured in the presence of Et_3N (5 equiv.) and Bu_4NOH (100 equiv.) respectively.

absorptions into the visible region. In the case of **2**, **3** and **6**, a similar band, albeit significantly less intense, is also observed in the spectra (***a*** in Figs. 8, S1 and S4) recorded before the addition of acid. This absorption indicates the co-existence in solution of a small fraction of ring-open isomer, together with the predominant ring-closed species, for these particular three switches.

The absorption spectra of **7** and **8** (***a*** in Figs. 9 and S5) are also indicative of the predominant presence of the ring-closed isomer in solution. In fact, they reveal bands at 428 and 320 nm respectively (Table 1), which resemble those of the model compounds **26** and **28** (***c*** in Fig. 9 and ***b*** in Fig. S5). Instead, there are no bands in the range of wavelengths where the phenolate chromophores of the ring-open isomers are expected to absorb, according to the spectra of the conjugate bases of the model phenols **27** and **18** (***d*** in Fig. 9 and ***c*** in Fig. S5). Nonetheless, a weak absorption for the phenolate chromophore can be detected at *ca.* 390 nm (***b*** in Fig. 9), after the addition of tetrabutylammonium hydroxide to **8**. Indeed, the oxazine ring of our compounds is known to open under these conditions with the formation of the corresponding hemiaminal (***d*** in Fig. 7) [15a, 16]. In the case of **7**, the nucleophilic hydroxide anion attacks also the 3*H*-indolium cation appended to the phenoxy fragment, in addition to opening the oxazine ring, and prevents the detection of the absorption band for the extended phenolate chromophore.

The steady-state emission spectra of **1**–**6** show negligible fluorescence and do not change significantly after the addition of acid. Similarly, also **7** and **8** (***e*** in Fig. 9) are essentially not emissive. After the addition of tetrabutylammonium hydroxide, however, a small fraction of the ring-closed isomer of **8** is converted into the corresponding hemiaminal (***d*** in Fig. 7) and an intense emission band appears at 470 nm (***f*** in Fig. 9) upon excitation at 405 nm. Indeed, the spectra of the model coumarin **28** (***g*** in Fig. 9) and of the conjugate base of the model phenol **18** (***h*** in Fig. 9) reveal that, while the former is virtually not emissive under these excitation conditions, the latter emits with a quantum yield of 0.99. Thus, the base-induced opening of the oxazine ring of **8** alters the electronic structure of the appended coumarin chromophore and switches its fluorescence from off to on.

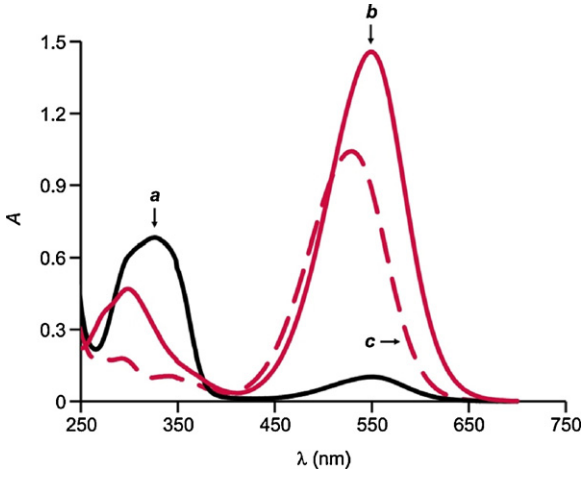

Fig. 8. Steady-state absorption spectra (50 μM, MeCN, 20 °C) of **2** before (***a***) and after (***b***) the addition of TFA (5 equiv.) and of the hexafluorophosphate salt of **21** (***c***).

2.3. Time-resolved spectroscopy

The steady-state absorption spectra (***a*** in Figs. 8, 9 and S1–S5) of **2**–**8** show that these molecular switches adopt preferentially the

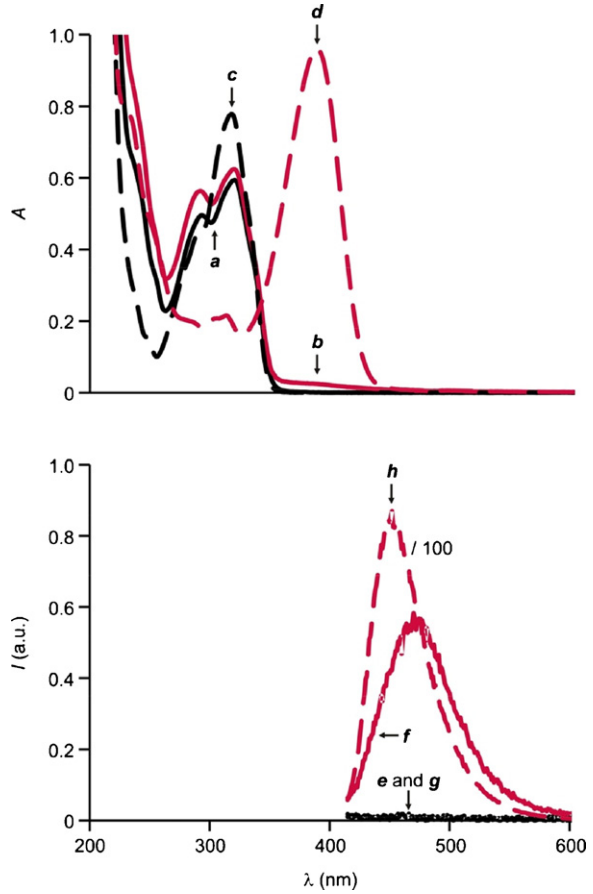

Fig. 9. Steady-state absorption spectra (50 μM, MeCN, 20 °C) of **8** before (***a***) and after (***b***) the addition of Bu_4NOH (100 equiv.), of **28** (***c***) and of **18** (***d***) after the addition of Bu_4NOH (100 equiv.). Steady-state emission spectra (50 μM, MeCN, 20 °C, λ_{Ex} = 405 nm) of **8** before (***e***) and after (***f***) the addition of Bu_4NOH (100 equiv.), of **28** (***g***) and of **18** (***h***) after the addition of Bu_4NOH (100 equiv).

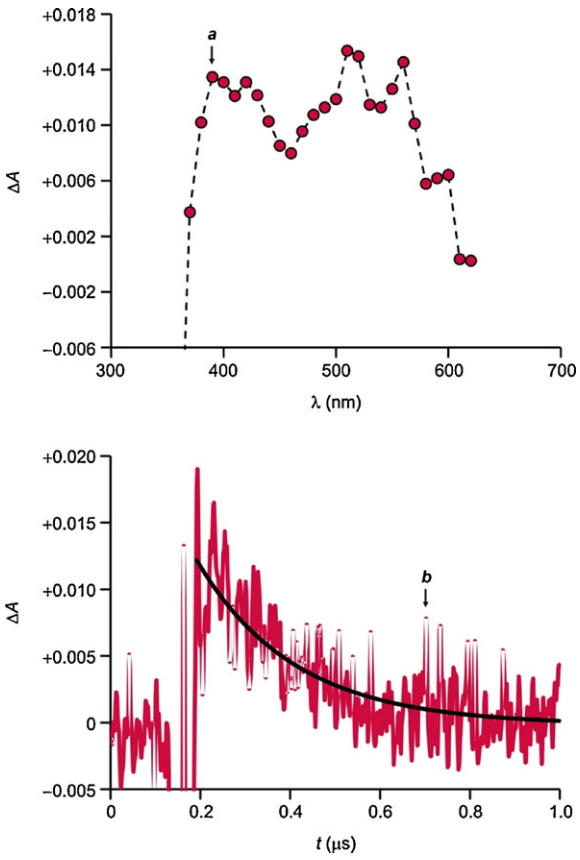

Fig. 10. Time-resolved absorption spectrum (***a***) of a solution (18 μM, MeCN, 20 °C) of **2**, recorded 0.1 μs after pulsed illumination at 355 nm (15 mJ, 6 ns), and the subsequent absorbance evolution (***b***) at 550 nm with the corresponding monoexponential fitting.

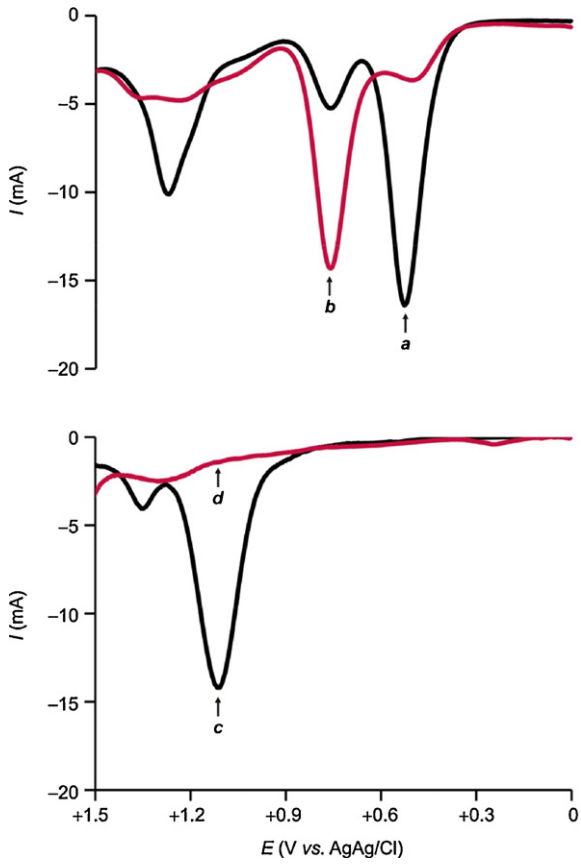

Fig. 11. Differential pulse voltammograms (1.5 mM, 0.1 M Bu_4NPF_6, MeCN, 20 °C, V *vs*. Ag/AgCl, scan rate = 20 mV s^{-1}, pulse amplitude = 50 mV) of **6** before (***a***) and after (***b***) the addition of TFA (1 equiv.) and of **9** before (***c***) and after (***d***) the addition of TFA (20 equiv).

ring-closed form (***a*** in Fig. 1) in acetonitrile at ambient temperature. Upon illumination at 355 nm with a pulsed laser, however, the oxazine ring of **2**, **3** and **5** opens within the duration of the laser pulse (6 ns) to generate the corresponding zwitterionic isomer (***b*** in Fig. 1) with a quantum yield (ϕ_P in Table 1) ranging from 0.01 to 0.03. Consistently, the absorption spectra (***a*** in Figs. 10, S6 and S8), recorded 0.1 μs after excitation, reveal the appearance of bands in the visible region. These bands resemble those observed in the steady-state spectra (***c*** in Figs. 8, S1 and S3) of the model compounds **21**, **22** and **24** and correspond to ground-state absorptions of the 3*H*-indolium chromophores of the ring-open isomers of **2**, **3** and **5**. The photogenerated isomers, however, revert spontaneously back to the original species and, consistently, their transient absorptions in the visible region decay monoexponentially (***b*** in Figs. 10, S6 and S8). Curve fitting of the resulting temporal absorbance profiles indicates the lifetime (τ_P in Table 1) to range from 0.2 to 50 μs. Interestingly, the lifetimes of the ring-open isomers of **3** and **5** are one order of magnitude longer than that of **2**. Presumably, their thiophene appendages stabilize effectively the 3*H*-indolium cation of the ring-open isomer, by extending its conjugation, and delay the ring-closing kinetics.

The time-resolved absorption spectra (***a*** in Figs. S7 and S9) of **4** and **6**, recorded under otherwise identical illumination conditions, also reveal an absorbance increase in the visible region. However, the resulting bands do not resemble those expected for the 3*H*-indolium cations of the corresponding ring-open isomers (***b*** in Figs. S2 and S4). The one observed for **4** is, instead, similar to the triplet–triplet absorption of bisthiophene [17] and its lifetime shortens from 2.7 to 0.3 μs in the presence of molecular oxygen (***b*** and ***c*** in Fig. S7). These observations suggest that intersystem crossing follows the excitation of **4** and prevents the opening of its oxazine ring. By contrast, the spectral changes observed upon irradiation of **6** are irreversible. Thus, this particular switch appears to undergo significant degradation under illumination. Presumably, intramolecular electron transfer pathways from the ferrocene appendage to the excited 4-nitrophenoxy chromophore are responsible for the photochemical decomposition of this compound.

In contrast to the behavior of **2**–**5**, the transient absorption spectra of **7** and **8** do not reveal any significant change on a nanosecond timescale upon illumination. The inability of their oxazine ring to open upon excitation on this temporal scale is, presumably, a result of the lack of a nitro group in position 4 of their phenoxy fragments. Indeed, all the structural modifications explored at this particular position so far, besides the introduction of either a nitro or a 4-nitrophenyl group, have translated in the suppression of the photochemical character of the oxazine ring [15d,j].

2.4. Differential pulse voltammetry

The steady-state absorption spectrum of **6** (***a*** in Fig. S4) reveals intense bands for the ring-closed isomer and a weak absorption for the ring-open species. In agreement with the co-existence of both isomers in solution, the differential pulse voltammogram of **6** (***a*** in Fig. 11) shows two peaks of different intensities at +0.52 and +0.76 V for the oxidation of the ferrocene fragments of the ring-closed and -open species respectively. Consistently with this assignment, the opening of the oxazine ring with acid (***a*** and ***c*** in Fig. 7) results in an increase in the intensity of peak at +0.76 V with a concomitant decrease in that at +0.52 V (***b*** in Fig. 11). Thus, the electrochemical

response of the redox center appended to the switchable unit can, indeed, be controlled by operating the latter with chemical inputs.

In addition to the two peaks for ferrocene oxidation, the differential pulse voltammogram of **6** shows also a third peak at +1.27 V (***a*** in Fig. 11). This peak resembles that observed for the model oxazine **9** (***c*** in Fig. 11) and corresponds to the oxidation of the 2*H*,3*H*-indole heterocycle. After the addition of acid and the opening of the oxazine ring, this particular fragment becomes positively charged, preventing the oxidation of the heterocyclic fragment, and the peak disappears for both compounds (***b*** and ***d*** in Fig. 11). Thus, the redox response of the switchable unit itself can also be controlled by opening the oxazine ring with chemical stimulations.

3. Conclusions

A switchable oxazine can be condensed to a variety of formylated chromophores in a single synthetic step. Either addition of acid or ultraviolet illumination opens the oxazine ring of the resulting constructs and brings the chromophoric fragment in conjugation with a 3*H*-indolium cation. This pronounced structural transformation extends the conjugation of the chromophore to shift its main absorption from the ultraviolet to the visible region and, in the case of a ferrocene center, also the oxidation potential in the positive direction. Alternatively, chromophoric fragments can be attached to the phenylene ring fused to the oxazine heterocycle. In this instance, the addition of base opens the oxazine ring and brings the chromophoric appendage in conjugation with a phenolate anion. Once again, this pronounced modification in electronic structure alters the absorption properties of the chromophore and, in the case of a coumarin fluorophore, leads also to a significant enhancement in emission intensity. Thus, this particular structural design to switch properties at the molecular level, coupled to the generality of the synthetic strategies, can facilitate the realization of functional materials able to respond to chemical inputs and optical stimulations.

4. Experimental procedures

4.1. Materials and methods

Chemicals were purchased from commercial sources and used as received with the exception of MeCN, which was distilled over CaH_2. Compounds **9**, **10**, **11**, **16**–**19** and **28** were prepared according to literature procedures [15a,g, 18–22]. Reactions were monitored by thin-layer chromatography, using aluminum sheets coated with silica. Electrospray ionization mass spectra (ESIMS) were recorded with a Bruker micrOTO-Q II spectrometer. Fast atom bombardment mass spectra (FABMS) were recorded with a VG Mass Lab Trio-2 spectrometer in a 3-nitrobenzyl alcohol matrix. Nuclear magnetic resonance (NMR) spectra were recorded with a Bruker Avance 400 spectrometer. Steady-state absorption spectra were recorded with a Varian Cary 100 Bio spectrometer, using quartz cells with a path length of 0.5 cm for **1**–**7** and their models and of 1.0 cm for **8** and its models. Steady-state emission spectra were recorded with a Varian Cary Eclipse spectrometer in aerated solutions. Fluorescence quantum yields were determined with fluorescein and rhodamine B standards, following a literature protocol [23]. Time-resolved absorption spectra were recorded with a Luzchem Research mLFP-111 spectrometer in aerated solutions by illuminating orthogonally the sample with a Continuum Surelite II-10 Nd:YAG pulsed laser. The quantum yields for the photochromic transformations were determined with a benzophenone standard, following a literature protocol [15k]. Differential pulse voltammograms were recorded with a CH Instruments 660 electrochemical analyzer under Ar, using a glassy-carbon working electrode (3 mm), a platinum counter electrode and a Ag/AgCl reference electrode.

4.2. Synthesis of *1*

A solution of **9** (100 mg, 0.3 mmol), **10** (151 mg, 1 mmol) and TFA (0.5 mL, 7 mmol) in MeCN (10 mL) was heated under reflux for 24 h. After cooling down to ambient temperature, the solvent was distilled off under reduced pressure and the residue was dissolved in CH_2Cl_2 (5 mL). The addition of Et_2O (50 mL) caused the precipitation of a solid, which was filtered off, dissolved in CH_2Cl_2 (20 mL) and washed with H_2O (20 mL). The organic phase was dried over Na_2SO_4 and the solvent was distilled off under reduced pressure to give **1** (50 mg, 35%) as a purple solid. ESIMS: m/z = 444.2287 $[M+H]^+$ (m/z calcd. for $C_{27}H_{30}N_3O_3$ = 444.2282); ^{1}H NMR ($CDCl_3$): δ = 1.10 (3H, t, 8 Hz), 1.73 (6H, s), 2.25 (3H, s), 2.42–2.48 (5H, m), 5.24 (2H, s), 6.44 (1H, d, 9 Hz), 7.25–7.29 (2H, m), 7.38–7.43 (2H, m), 7.64 (1H, d, 15 Hz), 7.77 (1H, s), 7.84–7.91 (2H, m).

4.3. Synthesis of *2*

A solution of **9** (155 mg, 0.5 mmol), **11** (191 mg, 0.7 mmol) and TFA (0.5 mL, 7 mmol) in EtOH (10 mL) was heated under reflux for 24 h. After cooling down to ambient temperature, the solvent was distilled off under reduced pressure and the residue was dissolved in CH_2Cl_2 (5 mL). The addition of Et_2O (50 mL) caused the precipitation of a solid, which was filtered off, dissolved in CH_2Cl_2 (20 mL) and washed with H_2O (20 mL). The organic phase was dried over Na_2SO_4 and the solvent was distilled off under reduced pressure to give **2** (119 mg, 42%) as a purple solid. ESIMS: m/z = 566.2445 $[M+H]^+$ (m/z calcd. for $C_{37}H_{32}N_3O_3$ = 566.2438); ^{1}H NMR ($CDCl_3$): δ = 1.41 (6H, bs), 4.60 (2H, s), 6.24 (1H, d, 16 Hz), 6.63 (1H, d, 8 Hz), 6.75 (1H, d, 16 Hz), 6.86–6.89 (2H, m), 7.00–7.15 (10H, m), 7.24–7.29 (6H, m), 7.96–8.02 (2H, m); ^{13}C NMR ($CDCl_3$): δ = 24.8, 41.2, 50.5, 109.2, 118.1, 119.7, 120.4, 122.7, 123.5, 123.6, 123.8, 124.5, 125.1, 125.5, 126.4, 126.7, 128.1, 128.2, 129.8, 130.0, 130.1, 131.7, 138.7, 140.9, 146.8, 147.6, 190.9.

4.4. Synthesis of *3*

A solution of **9** (300 mg, 1.0 mmol), **12** (89 μL, 1.0 mmol) and TFA (100 μL, 1.4 mmol) in EtOH (10 mL) was heated under reflux for 24 h. After cooling down to ambient temperature, the solvent was distilled off under reduced pressure and the residue was dissolved in CH_2Cl_2 (5 mL). The addition of Et_2O (50 mL) caused the precipitation of a solid, which was filtered off, dissolved in CH_2Cl_2 (20 mL) and washed with H_2O (20 mL). The organic phase was dried over Na_2SO_4 and the solvent was distilled off under reduced pressure to give **3** (100 mg, 26%) as a yellow solid. ESIMS: m/z = 405.1267 $[M+H]^+$ (m/z calcd. for $C_{23}H_{21}N_2O_3S$ = 405.1267); ^{1}H NMR ($CDCl_3$): δ = 1.28 (3H, bs), 1.59 (3H, bs), 4.59 (2H, s), 6.64 (1H, dd, 3 and 8 Hz), 6.87–6.92 (3H, m), 6.96–7.02 (2H, m), 7.10–7.15 (2H, m), 7.23 (1H, d, 5 Hz), 7.28 (1H, s), 7.97–8.01 (1H, m), 8.03 (1H, d, 3 Hz); ^{13}C NMR ($CDCl_3$): δ = 19.1, 23.1, 26.9, 41.1, 50.6, 103.9, 109.2, 118.1, 120.4, 121.2, 122.7, 123.7, 124.5, 126.0, 127.9, 128.1, 129.6, 138.5, 141.1, 146.7, 159.5.

4.5. Synthesis of *4*

A solution of **9** (250 mg, 0.8 mmol), **13** (156 mg, 0.8 mmol) and TFA (60 μL, 0.8 mmol) in EtOH (10 mL) was heated under reflux for 24 h. After cooling down to ambient temperature, the solvent was distilled off under reduced pressure and the residue was dissolved in CH_2Cl_2 (5 mL). The addition of Et_2O (50 mL) caused the precipitation of a solid, which was filtered off, dissolved in CH_2Cl_2 (20 mL) and washed with H_2O (20 mL). The organic phase was dried over

Na_2SO_4 and the solvent was distilled off under reduced pressure to give **4** (100 mg, 26%) as a purple solid. ESIMS: m/z = 487.1144 $[M+H]^+$ (m/z calcd. for $C_{27}H_{23}N_2O_3S_2$ = 487.1145); ^{1}H NMR ($CDCl_3$): δ = 1.57 (6H, bs), 4.63 (2H, s), 6.19 (1H, d, 5 Hz), 6.63 (1H, d, 4 Hz), 6.88 (4H, t, 7 Hz), 7.02–7.05 (2H, m), 7.10–7.18 (3H, m), 7.22 (1H, d, 4 Hz), 7.99 (1H, dd, 2 and 9 Hz), 8.03 (1H, s); ^{13}C NMR ($CDCl_3$): δ = 18.9, 25.8, 52.3, 54.1, 110.9, 115.1, 116.9, 120.9, 123.3, 125.1, 126.4, 127.7, 129.8, 135.9, 139.2, 140.7, 141.9, 143.4, 146.8, 148.5, 164.0.

4.6. Synthesis of **5**

A solution of **9** (180 mg, 0.6 mmol), **14** (65 mg, 0.6 mmol) and TFA (0.29 mL, 6.5 mmol) in EtOH (10 mL) was heated under reflux for 24 h. After cooling down to ambient temperature, the solvent was distilled off under reduced pressure and the residue was dissolved in CH_2Cl_2 (5 mL). The addition of hexane (50 mL) caused the precipitation of a solid, which was filtered off, dissolved in CH_2Cl_2 (20 mL) and washed with H_2O (20 mL). The organic phase was dried over Na_2SO_4 and the solvent was distilled off under reduced pressure. The residue was purified by preparative thin-layer chromatography [SiO_2: AcOEt/hexanes (3:7, v/v)] to give **5** (100 mg, 42%) as a yellow oil. ESIMS: m/z = 405.1266 $[M+H]^+$ (m/z calcd. for $C_{23}H_{20}N_2O_3S$ = 405.1267); ^{1}H NMR ($CDCl_3$): δ = 1.57 (6H, s), 4.59 (2H, s), 5.31 (1H, s), 6.18 (1H, d, 16 Hz), 6.62 (1H, d, 7 Hz), 6.79–6.89 (3H, m), 7.12–7.14 (1H, t, 4 Hz), 7.23 (1H, bs), 7.25–7.27 (1H, bs), 7.30 (1H, d, 3 Hz), 7.98–8.02 (2H, m).

4.7. Synthesis of **6**

A solution of **9** (150 mg, 0.5 mmol), **15** (104 mg, 0.5 mmol) and TFA (0.24 mL, 6.5 mmol) in EtOH (10 mL) was heated under reflux and Ar for 24 h. After cooling down to ambient temperature, the solvent was distilled off under reduced pressure and the residue was dissolved in CH_2Cl_2 (5 mL). The addition of hexanes (50 mL) caused the precipitation of a solid, which was filtered off, dissolved in CH_2Cl_2 (20 mL) and washed with H_2O (20 mL). The organic phase was dried over Na_2SO_4 and the solvent was distilled off under reduced pressure. The residue was dissolved in EtOAc (10 mL) and filtered through a SiO_2 plug. The plug was washed with EtOAc (100 mL) and the solvent of the filtrate was distilled off under reduced pressure to give **6** (100 mg, 40%) as a dark-green solid. ESIMS: m/z = 507.1387 $[M+H]^+$ (m/z calcd. for $C_{29}H_{26}FeN_2O_3$ = 507.1366); ^{1}H NMR (CD_3CN): δ = 1.38 (6H, bs), 3.95 (5H, s), 4.42 (2H, s), 4.46 (2H, s), 4.71 (2H, s), 5.46 (1H, s), 6.05 (1H, d, 16 Hz), 6.70–7.20 (5H, m), 8.01 (1H, bs), 8.13 (1H, bs).

4.8. Synthesis of the hexafluorophosphate salt of **7**

A mixture of **16** (142 mg, 0.4 mmol) and the iodide salt of **17** (100 mg, 0.3 mmol) in EtOH (20 mL) was heated under reflux for 24 h. After cooling down to ambient temperature, the solvent was distilled off under reduced pressure and the residue was dissolved in CH_2Cl_2 (5 mL). The addition of Et_2O (50 mL) caused the precipitation of a solid, which was filtered off, and dissolved in Me_2CO (5 mL). After the addition of a saturated aqueous solution of NH_4PF_6 (5 mL), the solution was concentrated under reduced pressure to half of its original volume and the resulting precipitate was filtered off to give the hexafluorophosphate salt of **7** (100 mg, 46%) as an orange powder. ESIMS: m/z = 511.2760 $[M-PF_6]^+$ (m/z calcd. for $C_{36}H_{35}N_2O$ = 511.2744); ^{1}H NMR ($CDCl_3$): δ = 0.78 (3H, s), 1.56 (3H, s), 1.71 (6H, s), 4.22 (3H, s), 4.53 (1H, d, 18 Hz), 5.02 (1H, d, 18 Hz), 6.72–6.82 (2H, m), 6.90 (1H, d, 8 Hz), 7.07 (2H, q, 8 Hz), 7.25–7.40 (3H, m), 7.44 (4H, s), 7.55–7.64 (5H, m), 8.06 (1H, d, 16 Hz), 8.50 (1H, s); ^{13}C NMR ($CDCl_3$): δ = 18.2, 25.7, 27.4, 34.2, 40.6, 49.8, 52.7, 105.5, 109.7, 110.6, 115.1, 119.0, 121.0, 122.7, 123.1, 127.6, 128.0, 128.5, 128.9, 129.3, 129.6, 129.7, 130.9, 131.0, 136.6, 138.0, 142.6, 143.9, 147.7, 154.4, 159.2, 182.7, 205.2, 205.7, 206.1.

4.9. Synthesis of **8**

An aqueous solution of formaldehyde (37%, 0.81 mL, 10 mmol) was added dropwise to a suspension of **18** (880 mg, 5 mmol) in HCl_{conc} (8 mL). The mixture was stirred at 40 °C for 4 h and, after cooling down to ambient temperature, diluted with H_2O (20 mL). The resulting precipitate was filtered off, washed with H_2O (20 mL) dissolved in MeCN (20 mL) together with **19** (721 mg, 3 mmol). The mixture was heated for 24 h under reflux. After cooling down to ambient temperature, the solvent was distilled off under reduced pressure and the residue was dissolved in CH_2Cl_2 (20 mL). The resulting solution was washed with H_2O (2 × 20 mL). The solvent of the organic phase was distilled off under reduced pressure and the residue was purified by column chromatography [SiO_2: CH_2Cl_2] to afford **8** (650 mg, 16%) as a white solid. ESIMS: m/z = 410.1751 $[M+H]^+$ (m/z calcd. for $C_{27}H_{24}NO_3$ = 410.1747); ^{1}H NMR ($CDCl_3$): δ = 0.85 (3H, s), 1.61 (3H, s), 2.28 (3H, s), 4.51 (1H, d, 16 Hz), 4.99 (1H, d, 16 Hz), 6.05 (1H, s), 6.79 (2H, d, 8 Hz), 6.89 (1H, t, 8 Hz), 7.14–7.18 (2H, m), 7.26 (1H, d, 8 Hz), 7.32–7.41 (3H, m), 7.67 (2H, bs); ^{13}C NMR ($CDCl_3$): δ = 18.8, 18.9, 19.1, 37.2, 104.8, 108.5, 109.1, 109.8, 111.8, 111.9, 113.4, 114.3, 120.5, 128.5, 128.5, 128.9, 129.1, 129.2, 136.5, 137.9, 147.7, 151.9, 153.4, 157.0, 161.4.

4.10. Synthesis of the hexafluorophosphate salt of **20**

A solution of **10** (200 mg, 0.9 mmol) and the iodide salt of **17** (240 mg, 0.8 mmol) in EtOH (10 mL) was heated under reflux for 24 h. After cooling down to ambient temperature, the solvent was distilled off under reduced pressure and the residue was dissolved in CH_2Cl_2 (5 mL). The addition of Et_2O (30 mL) caused the precipitation of a solid, which was filtered off and dissolved in Me_2CO (5 mL). After the addition of a saturated aqueous solution of NH_4PF_6 (5 mL), the solution was concentrated under reduced pressure to half of its original volume and the resulting precipitate was filtered off to give the hexafluorophosphate salt of **20** (235 mg, 65%) as a purple solid. FABMS: m/z = 307 $[M-PF_6]^+$ (m/z calcd. for $C_{21}H_{27}N_2$ = 307); ^{1}H NMR ($CDCl_3$): δ = 1.08 (3H, t, 7 Hz), 1.71 (6H, s), 2.45 (3H, s), 2.42 (2H, q, 7 Hz), 2.64 (3H, s), 4.00 (3H, s), 7.17 (1H, d, 8 Hz), 7.30 (1H, d, 9 Hz), 7.37–7.45 (2H, m), 7.50 (1H, d, 15 Hz), 7.66 (1H, d, 15 Hz), 12.47 (1H, bs); ^{13}C NMR ($CDCl_3$): δ = 10.2, 12.3, 15.0, 17.7, 28.6, 32.3, 50.0, 98.7, 11.8, 122.5, 126.7, 129.4, 129.8, 130.7, 135.1, 38.6, 141.3, 142.8, 150.1, 176.9.

4.11. Synthesis of the hexafluorophosphate salt of **21**

A solution of **11** (300 mg, 1 mmol) and the iodide salt of **17** (300 mg, 1 mmol) in EtOH (10 mL) was heated under reflux for 24 h. After cooling down to ambient temperature, the solvent was distilled off under reduced pressure and the residue was dissolved in CH_2Cl_2 (5 mL). The addition of Et_2O (30 mL) caused the precipitation of a solid, which was filtered off and dissolved in Me_2CO (5 mL). After the addition of a saturated aqueous solution of NH_4PF_6 (5 mL), the solution was concentrated under reduced pressure to half of its original volume and the resulting precipitate was filtered off to give the hexafluorophosphate salt of **21** (184 mg, 32%) as a purple solid. ESIMS: m/z = 429 $[M]^+$ (m/z calcd. for $C_{31}H_{29}N_2$ = 429); ^{1}H NMR ($CDCl_3$): δ = 1.82 (6H, s), 4.35 (3H, s), 2.45 (3H, s), 7.02 (2H, d, 9 Hz), 7.20 (2H, d, 8 Hz), 7.24 (2H, t, 7 Hz), 7.38 (5H, t, 8 Hz), 7.46–7.56 (5H, m), 7.61 (1H, d, 16 Hz), 8.02 (2H, d, 9 Hz), 8.08 (1H, d, 16 Hz); ^{13}C NMR ($CDCl_3$): δ = 27.3, 33.9, 52.2, 107.5, 114.1, 119.7, 122.8, 126.5, 126.7, 127.0, 129.2, 129.8, 130.3, 133.6, 142.0, 142.9, 145.6, 154.2, 154.7, 181.1.

4.12. Synthesis of the hexafluorophosphate salt of **22**

A solution of **12** (77 μL, 0.8 mmol) and the iodide salt of **17** (250 mg, 0.8 mmol) in EtOH (10 mL) was heated under reflux for 24 h. After cooling down to ambient temperature, the solvent was distilled off under reduced pressure and the residue was dissolved in CH_2Cl_2 (5 mL). The addition of Et_2O (30 mL) caused the precipitation of a solid, which was filtered off and dissolved in Me_2CO (5 mL). After the addition of a saturated aqueous solution of NH_4PF_6 (5 mL), the solution was concentrated under reduced pressure to half of its original volume and the resulting precipitate was filtered off to give the hexafluorophosphate salt of **22** (80 mg, 24%) as a brown solid. FABMS: m/z = 268 $[M-PF_6]^+$ (m/z calcd. for $C_{17}H_{18}NS$ = 268); ^{1}H NMR ($CDCl_3$): δ = 1.87 (6H, s), 4.39 (3H, s), 7.29 (1H, s), 7.40 (1H, d, 16 Hz), 7.55–7.61 (4H, m), 7.82 (1H, d, 5 Hz), 8.34 (1H, s), 8.51 (1H, d, 16 Hz).

4.13. Synthesis of the hexafluorophosphate salt of **23**

A solution of **13** (161 mg, 0.8 mmol) and the iodide salt of **17** (250 mg, 0.8 mmol) in EtOH (10 mL) was heated under reflux for 24 h. After cooling down to ambient temperature, the solvent was distilled off under reduced pressure and the residue was dissolved in CH_2Cl_2 (5 mL). The addition of Et_2O (30 mL) caused the precipitation of a solid, which was filtered off and dissolved in Me_2CO (5 mL). After the addition of a saturated aqueous solution of NH_4PF_6 (5 mL), the solution was concentrated under reduced pressure to half of its original volume and the resulting precipitate was filtered off to give the hexafluorophosphate salt of **23** (100 mg, 25%) as a brown solid. FABMS: m/z = 351 $[M-PF_6]^+$ (m/z calcd. for $C_{21}H_{20}NS_2$ = 350); ^{1}H NMR ($CDCl_3$): δ = 1.86 (6H, s), 4.32 (3H, s), 7.10–7.13 (1H, m), 7.20–7.24 (1H, m), 7.34 (1H, d, 4 Hz), 7.42–7.46 (2H, m), 7.53–7.56 (4H, m), 8.37 (1H, d, 4 Hz), 8.53 (1H, d, 15 Hz).

4.14. Synthesis of the hexafluorophosphate salt of **24**

A solution of **14** (116 mg, 1.0 mmol) and the iodide salt of **17** (180 mg, 1.0 mmol) in EtOH (10 mL) was heated under reflux for 24 h. After cooling down to ambient temperature, the solvent was distilled off under reduced pressure and the residue was dissolved in CH_2Cl_2 (5 mL). The addition of Et_2O (30 mL) caused the precipitation of a solid, which was filtered off and dissolved in Me_2CO (5 mL). After the addition of a saturated aqueous solution of NH_4PF_6 (5 mL), the solution was concentrated under reduced pressure to half of its original volume and the resulting precipitate was filtered off to give the hexafluorophosphate salt of **24** (100 mg, 36%) as a brown solid. ESIMS: m/z = 268 $[M]^+$ (m/z calcd. for $C_{17}H_{18}NS$ = 268); ^{1}H NMR ($CDCl_3$): δ = 1.79 (6H, s), 4.35 (3H, s), 7.47–7.63 (6H, m), 7.88 (1H, s), 8.23 (1H, d, 17 Hz), 8.36 (1H, s); ^{13}C NMR [$(CD_3)_2CO$]: δ = 25.2, 34.1, 52.6, 112.4, 114.9, 122.8, 125.8, 128.6, 129.3, 129.6, 136.5, 138.8, 142.2, 143.6, 147.4, 183.0.

4.15. Synthesis of the hexafluorophosphate salt of **26**

A solution of 4-methoxybenzaldehyde (68 mg, 0.5 mmol) and the iodide salt of **17** (100 mg, 0.3 mmol) in EtOH (20 mL) was heated under reflux for 24 h. After cooling down to ambient temperature, the solvent was distilled off under reduced pressure and the residue was dissolved in CH_2Cl_2 (5 mL). The addition of Et_2O (30 mL) caused the precipitation of a solid, which was filtered off and dissolved in Me_2CO (5 mL). After the addition of a saturated aqueous solution of NH_4PF_6 (5 mL), the solution was concentrated under reduced pressure to half of its original volume and the resulting precipitate was filtered off to give the hexafluorophosphate salt of **26** (120 mg, 83%) as a yellow-orange solid. ESIMS: m/z = 292 $[M-PF_6]^+$ (m/z calcd. for $C_{20}H_{22}NO$ = 292); ^{1}H NMR [$(CD_3)_2CO$]: δ = 1.85 (6H, s), 3.92 (3H, s), 4.45 (3H, s), 7.07 (2H, d, 8 Hz), 7.54 (2H, s), 7.57 (2H, s), 7.78 (1H, d, 16 Hz), 8.18 (1H, d, 16 Hz), 8.23 (2H, d, 8 Hz); ^{13}C NMR ($CDCl_3$): δ = 25.8, 34.2, 52.8, 55.8, 110.5, 115.1, 115.5, 115.7, 123.2, 127.8, 129.6, 129.7, 133.4, 142.6, 143.9, 154.5, 165.1, 182.8.

4.16. Synthesis of the hexafluorophosphate salt of **27**

A solution of 4-hydroxybenzaldehyde (61 mg, 0.5 mmol) and the iodide salt of **17** (100 mg, 0.3 mmol) in EtOH (20 mL) was heated under reflux for 24 h. After cooling down to ambient temperature, the solvent was distilled off under reduced pressure and the residue was dissolved in CH_2Cl_2 (5 mL). The addition of Et_2O (30 mL) caused the precipitation of a solid, which was filtered off and dissolved in Me_2CO (5 mL). After the addition of a saturated aqueous solution of NH_4PF_6 (5 mL), the solution was concentrated under reduced pressure to half of its original volume and the resulting precipitate was filtered off to give the hexafluorophosphate salt of **27** (110 mg, 78%) as a yellowish-orange solid. ESIMS: m/z = 278 $[M-PF_6]^+$ (m/z calcd. for $C_{19}H_{20}NO$ = 278); ^{1}H NMR [$(CD_3)_2CO$]: δ = 1.85 (6H, s), 4.12 (3H, s), 6.98 (2H, d, 9 Hz), 7.44 (1H, d, 9 Hz), 7.61–7.66 (2H, m), 7.43–7.81 (2H, m), 8.00 (2H, d, 9 Hz), 8.39 (1H, d, 16 Hz); ^{13}C NMR [$(CD_3)_2CO$]: δ = 25.9, 34.1, 52.7, 109.7, 114.9, 117.0, 123.1, 126.9, 129.6, 133.8, 142.6, 143.8, 154.9, 163.7, 182.7, 205.5.

Acknowledgments

FMR thanks the National Science Foundation (CAREER Award CHE-0237578, CHE-0749840 and CHE-1049860) for supporting his research program and for providing funds to purchase a mass spectrometer (CHE-0946858). SS thanks the MIUR (PRIN 2008) for financial support and the Royal Society of Chemistry for a travel grant.

Appendix A. Supplementary data

Supplementary data associated with this article can be found, in the online version, at doi:10.1016/j.jphotochem.2011.11.008.

References

[1] B.L. Feringa, W.R. Browne (Eds.), Molecular Switches, Wiley-VCH, Weinheim, 2011.
[2] V. Balzani, M. Venturi, A. Credi, Molecular Devices and Machines: Concepts and Perspectives for the Nanoworld, Wiley-VCH, Weinheim, 2008.
[3] G.H. Dorion, A.F. Wiebe, Photochromism, Focal Press, New York, 1970.
[4] G.H. Brown (Ed.), Photochromism, Wiley, New York, 1971.
[5] A.V. El'tsov (Ed.), Organic Photochromes, Consultants Bureau, New York, 1990.
[6] H. Bouas-Laurent, H. Dürr (Eds.), Photochromism: Molecules and Systems, Elsevier, Amsterdam, 1990.
[7] J.C. Crano, R. Guglielmetti (Eds.), Organic Photochromic and Thermochromic Compounds, Plenum Press, New York, 1999.
[8] M. Irie (Ed.), Chem. Rev. 100 (2000) 1683–1890.
[9] K. Matsuda, M.J. Irie, Photochem. Photobiol. C 5 (2004) 169–182.
[10] H. Tian, S.J. Yang, Chem. Soc. Rev. 33 (2004) 85–97.
[11] D. Gust, T.A. Moore, A.L. Moore, Chem. Commun. (2006) 1169–1178.
[12] H.D. Samachetty, N.R. Branda, Pure Appl. Chem. 78 (2006) 2351–2359.
[13] M.-M. Russew, S. Hecht, Adv. Mater. 22 (2010) 3348–3360.
[14] (a) F.M. Raymo, Angew. Chem. Int. Ed. 45 (2006) 5249–5251;
(b) F.M. Raymo, M. Tomasulo, Chem. Eur. J. 12 (2006) 3186–3193.
[15] (a) M. Tomasulo, S. Sortino, A.J.P. White, F.M. Raymo, J. Org. Chem. 70 (2005) 8180–8189;
(b) M. Tomasulo, S. Sortino, F.M. Raymo, Org. Lett. 7 (2005) 1109–1112;
(c) M. Tomasulo, F.M. Raymo, Org. Lett. 7 (2005) 4633–4636;
(d) M. Tomasulo, S. Sortino, A.J.P. White, F.M. Raymo, J. Org. Chem. 71 (2006) 744–753;
(e) M. Tomasulo, S. Sortino, F.M. Raymo, Asian Chem. Lett. 11 (2007) 219–222;
(f) M. Tomasulo, S. Sortino, F.M. Raymo, Adv. Mater. 20 (2008) 832–835;
(g) M. Tomasulo, S. Sortino, F.M. Raymo, J. Org. Chem. 73 (2008) 118–126;
(h) M. Tomasulo, S. Sortino, F.M. Raymo, J. Photochem. Photobiol. A 200 (2008) 44–49;
(i) M. Tomasulo, E. Deniz, T. Benelli, S. Sortino, F.M. Raymo, Adv. Funct. Mater. 19 (2009) 3956–3961;
(j) M. Åxman Petersen, E. Deniz, M. Brøndsted Nielsen, S. Sortino, F.M. Raymo, Eur. J. Org. Chem. (2009) 4333–4339;

(k) E. Deniz, M. Tomasulo, S. Sortino, F.M. Raymo, J. Phys. Chem. C 113 (2009) 8491–8497;
(l) M. Tomasulo, E. Deniz, S. Sortino, F.M. Raymo, Photochem. Photobiol. Sci. 9 (2010) 136–140;
(m) E. Deniz, S. Ray, M. Tomasulo, S. Impellizzeri, S. Sortino, F.M. Raymo, J. Phys. Chem. A 114 (2010) 11567–11575;
(n) E. Deniz, S. Sortino, F.M. Raymo, J. Phys. Chem. Lett. 1 (2010) 1690–1693;
(o) E. Deniz, S. Sortino, F.M. Raymo, J. Phys. Chem. Lett. 1 (2010) 3506–3509;
(p) E. Deniz, S. Impellizzeri, S. Sortino, F.M. Raymo, Can. J. Chem. 89 (2011) 110–116;
(q) E. Deniz, M. Tomasulo, J. Cusido, S. Sortino, F.M. Raymo, Langmuir 27 (2011) 11773–11783.

[16] The absorbance at 390 nm (***b*** in Fig. 9) together with the molar extinction coefficient of the model phenolate (***d*** in Fig. 9) indicate that the addition of 100 equiv. of tetrabutylammonium hydroxide converts *ca.* 3% of **8** into the corresponding hemiaminal (***d*** in Fig. 7).

[17] M. Montalti, A. Credi, L. Prodi, M.T. Gandolfi, Handbook of Photochemistry, CRC Press, Boca Raton, 2006.

[18] The synthesis of **9** was originally reported in:
(a) A.A. Shachkus, J. Degutis, A. Jezerskaite, in: J. Kovac, P. Zalupsky (Eds.), Chemistry of Heterocyclic Compounds, vol. 35, Elsevier, Amsterdam, 1987, pp. 518–520;
(b) A.A. Shachkus, J. Degutis, A.G. Urbonavichyus, Khim. Geterotskil. Soed. 5 (1989) 672–676;
A.A. Shachkus, J. Degutis, A.G. Urbonavichyus, Chem. Heterocycl. Compd. (1989) 562–565.

[19] S.E. Bioadjiev, D.A. Lightner, Tetrahedron 55 (1999) 10871–10886.

[20] H. Tian, X. Yang, R. Chen, R. Zhang, A. Hagfeldt, L. Sun, J. Phys. Chem. C 112 (2008) 11023–11033.

[21] E. Hejchman, D. Maciejewska, I. Wolska, Monatsh. Chem. 139 (2008) 1337–1348.

[22] S. Cavar, F. Kovac, M. Maksimovic, Food Chem. 117 (2009) 135–142.

[23] J.R. Lakowicz, Principles of Fluorescence Spectroscopy, Springer, New York, 2006.